Cell Death and Differentiation (2007) 14, 489–499

www.nature.com/cdd

Granzyme K cleaves the nucleosome assembly protein SET to induce single-stranded DNA nicks of target cells

T Zhao[1], H Zhang[1], Y Guo[1], Q Zhang[1], G Hua[1], H Lu[1], Q Hou[1], H Liu[1] and Z Fan*[,1]

Although granzymes (Gzms) A- and B-induced cell death pathways have been defined, little is known about how other orphan Gzms function in CTL-mediated cytotoxicity. GzmK and A are tryptases among all the Gzms of humans and they are closely linked on the same chromosome. In this study, we showed that GzmK can be efficiently delivered into target cells with a cationic lipid protein transfection reagent Pro-Ject. We found human GzmK triggers rapid cell death independently of caspase activation. The features of death are characterized by rapid externalization of phosphatidylserine, nuclear morphological changes and single-stranded DNA nicks. GzmK hydrolyzes the nucleosome assembly protein SET in its recombinant and native forms or in intact cells. Cleavage of SET by GzmK abrogates its nucleosome assembly activity. After GzmK loading, SET and DNase NM23H1 rapidly translocate into the nucleus and SET is cleaved, where the nuclease activity of NM23H1 is activated to nick chromosomal DNA.
Cell Death and Differentiation (2007) **14,** 489–499. doi:10.1038/sj.cdd.4402040; published online 29 September 2006

Granule-mediated cytotoxicity is the major pathway for killer lymphocytes to kill viruses, intracellular bacteria and transformed cells.[1,2] After a killer lymphocyte recognizes its target, the cytotoxic granules move to the immunological synapse by exocytosis, where their membrane fuses with the killer cell plasma membrane, then they release their contents into the target cell by endocytosis.[3,4] Cytotoxic granules contain a pore-forming protein (PFP) perforin and a group of serine proteases termed granzymes (Gzms) in a proteoglycan matrix.[5,6] PFP helps Gzm uptake and appears to contribute to the release of Gzms from endosomal vesicles.[1,7] Gzms are serine esterases and different from the target membrane-disrupting proteins or granulysin present in the same granules. PFP delivers Gzms to initiate target cell apoptosis. Up to date, nine mouse, eight rat and five human Gzms have been described.[8] GzmA and B are the most abundant members of the Gzm family in humans and mice and have been most extensively studied.[9,10] However, little is known about the functions and mechanisms of other Gzms, so called as orphan Gzms.[8] The orphan Gzms include GzmH, K and M in humans.

GzmA is the most abundant protease in the cytotoxic granules, whose expression is constitutive in many NK cells and is initiated about 3–5 days after naïve T cells are induced to differentiate into CTL through activation.[11] GzmA has a trypsin-like activity and cleaves its specific substrates after basic residues Arg or Lys. GzmA induces single-stranded DNA nicks and a caspase-independent pathway via destruction of an endoplasmic reticulum (ER)-associated SET complex.[9] A recent report showed that GzmA triggers a rapid increase in reactive oxygen species (ROS) and mitochondrial transmembrane potential loss.[12] GzmB is a caspase-like serine protease that cuts substrates post-aspartic acid residues. GzmB causes double-stranded DNA fragmentation and caspase-dependent and independent cell death.[10] GzmA- or B-deficient mice were compromised in their abilities to eliminate only some certain virus infections and mildly susceptible compared with wide-type mice.[13,14] However, GzmA and B double-deficient mice were 1000-fold more susceptible than the single gene knockout mice. It indicates GzmA and B have synergistic action in viral clearance but they are not sufficient for killing a wide variety of viruses against infections. A recent report showed that GzmM induces a caspase-independent death pathway different from GzmA and B.[15] Another group showed that murine orphan GzmC induces cell death by attacking nuclei and mitochondria.[16] These suggest that multiple Gzms are needed to trigger cytolysis for providing backup and failsafe mechanisms for killing various pathogens and tumor cells.

GzmK and A are the two tryptases among all the Gzms and they are closely linked together on the same chromosome of humans and mice. Complete inhibition of tryptase activity by specific inhibitor abolishes CD8+ response against pathogens.[17] It suggests that tryptase is essential for CTL-mediated cytolysis. GzmA-deficient CTL has only a slightly reduced cytolytic activity against allogeneic targets.[18] These CTLs still contain 20% tryptase activity. GzmA-deficient CTL did not alter GzmK gene and its expression. GzmK is the alternate tryptase and may be a potent Gzm to rescue the GzmA function with redundant specificity. GzmK is much less abundant in human lymphokine-stimulated killer cell granules than GzmA.[19] Whereas GzmK is significantly higher amount in rat NK tumor cell line RNK-16. One report showed that rat GzmK, known as fragmentin-3, induces DNA fragmentation

[1]National Laboratory of Biomacromolecules and Center for Infection and Immunity, Institute of Biophysics, Chinese Academy of Sciences, Beijing, China
*Corresponding author: Z Fan, National Laboratory of Biomacromolecules and Center for Infection and Immunity, Institute of Biophysics, Chinese Academy of Sciences, Beijing 100101, China. Tel: +010 64888457; Fax: +010 64871293; E-mail: fanz@moon.ibp.ac.cn
Keywords: granzyme K; SET; apoptosis; DNA nicking; mechanism
Abbreviations: Gzm, granzyme; NAP, nucleosome assembly protein; PJ, Pro-Ject; PFP, pore forming protein; GAAD, GzmA-activated DNase; IGAAD, inhibitor of GAAD; Ad, adenovirus
Received 18.1.06; revised 09.8.06; accepted 10.8.06; Edited by JA Trapani; published online 29.9.06

without apoptotic nuclear morphology, but with disruption of the mitochondrial potential and dysfunction.[20,21] However, it is unknown about how human GzmK works and which physiological substrates it utilizes in granule-mediated apoptosis. Perforin triggers a rapid endocytosis of Gzms into target cells, where Gzms release into cytosol from the endosome with the help of perforin and activate apoptosis.[22] Cationic lipid protein transfection reagent Pro-Ject (PJ) can transport biologically active molecules into target cells by endocytosis and release them into cytosol,[23] which is reminiscent of Gzms delivery into cytosol by perforin. In this study, we expressed human active GzmK and its inactive form S-AGzmK. We used PJ to transport GzmK into target cells to define its function in granule-induced cytolysis. We found human GzmK induces rapid caspase-independent cell death with chromatin condensation and apoptotic nuclear morphology analogous to GzmA. GzmK degrades the nucleosome assembly protein (NAP) SET and disrupts its normal NAP function. GzmK activates the DNase activity of the GzmA-activated DNase (GAAD) NM23H1 to nick chromosomal DNA by degradation of its inhibitor (IGAAD) SET.

Results

GzmK induces rapid caspase-independent cell death. To determine the roles of human GzmK in granule-mediated cell death, we expressed human active GzmK in *Escherichia coli* and purified it from bacterial lysates by nickel chelation chromatography. The inactive form S-AGzmK was generated by mutation of the active site serine 214 to Ala. The enzymatic specificity of rGzmK was detected by measuring the hydrolysis of thioester substrates Z-Lys-SBzl as assayed for human rGzmA and rGzmK.[24–26] Active rGzmK appeared strongly proteolytic activity, whereas S-AGzmK had not (data not shown). A report showed that native rat GzmK triggers slow acting DNA fragmentation without apoptotic nuclear morphology.[20] We wanted to look at how human GzmK targets cell death. A cationic lipid-based protein transfection reagent PJ (Pierce Biotechnology) was used to deliver GzmK into target cells. PJ is utilized to deliver biologically active proteins directly into living cells. Proteins loaded by PJ remain biologically active, as the interaction between a protein and PJ is non-covalent. An optimal dose of PJ was used to load GzmA or B into target cells, which led to similar apoptotic morphological features as PFP-delivered GzmA or B within 4 h (data not shown). To detect whether human GzmK induces cytolysis, 2 μM GzmK was added with PJ into ^{51}Cr-labeled Jurkat or HeLa cells for 4 h standard specific cytotoxicity assay. In three independent experiments, GzmK plus PJ induced 84$\pm$4 and 39$\pm$3% specific lysis in Jurkat and HeLa cells, respectively (Figure 1a). GzmK and PJ alone or S-AGzmK plus PJ just got background lysis (generally $<$10%). The cell death induced by GzmK was also observed by trypan blue uptake (data not shown).

To further characterize the death features induced by GzmK, we next analyzed phosphatidylserine externalization through staining with the vital dye propidium iodide (PI) and Fluos-coupled Annexin V. The externalization of phosphatidylserine is a further hallmark of the apoptotic cells. Cells undergoing apoptosis transit from an early-stage Annexin V$^+$/PI$^-$ to a late-stage Annexin V$^+$/PI$^+$. A 2 μM portion of GzmK loading with PJ induced 31% Annexin V$^+$/PI$^+$ cells after 4 h (Figure 1c). A 1 μM portion of caspase 3 was delivered into cells as a positive control and got 34.3% Annexin V$^+$/PI$^+$ cells. GzmK and PJ alone or inactive S-AGzmK plus PJ were just got background Annexin V$^+$/PI$^+$ cells.

To compare the efficient delivery of GzmK by PJ or PFP, 2×10^5 Jurkat cells were treated with different concentrations of GzmK in the presence of sublytic PFP (10 nM) or the optimal dose of PJ at 37°C for 4 h. A 0.1 μM portion of GzmK began to induce significant death and dynamically augmented with increasing concentrations of GzmK (Annexin V$^+$/PI$^+$ cells: 15.3, 17.9 and 23%) (Figure 1d). GzmK and PFP alone or inactive S-AGzmK plus PFP got comparable death (generally less than 10%). A 0.5 μM portion of GzmK started to mediate apparent death that was analogous to that induced by PFP loaded GzmK. GzmK plus PFP got a higher proportion of single-positive PI cells than that induced by GzmK with PJ at the same enzymatic concentrations by 4 h. High concentration of GzmK (2 μM) plus PJ or incubation for longer time (6 h) obtained similar proportion of single-positive PI cells to that of GzmK (1 μM) plus PFP (data not shown). This indicates GzmK does not induce typical apoptosis and PFP has more efficient delivery of Gzms into target cells than PJ. The data are representative of at least three independent experiments. Similar results were found in HeLa cells (data not shown). We showed here that the amount of GzmK loaded by PJ in the induction of death was 10-fold greater than the concentration required to induce the similar rate of death in the presence of PFP. We utilized PJ to load GzmA or B into target cells that led to similar apoptotic features and cleavage of their substrates as PFP or adenovirus (Ad) delivered GzmA or B (data not shown). Therefore, PJ is able to imitate PFP for loading Gzms into target cells *in vitro*.

GzmK and A hold tryptase activity among all the human Gzms. GzmA induces cell death independently of caspase activation.[27,28] We next wanted to assess whether cell death triggered by human GzmK is dependent on caspase activity or not. Preincubation of cells with the broad caspase inhibitor ZVAD-fmk (100 μM) did not significantly inhibit GzmK-induced specific cytolysis compared with that of GzmK loading plus PJ (84$\pm$4 and 70$\pm$2%, respectively, $P>0.05$) (Figure 1a). However, the same concentration of ZVAD-fmk blocked GzmB-induced cytotoxicity distinctively (28 *versus* 8.3%) (Figure 1c). ZVAD-fmk (100 μM) was without effect on the externalization of phosphatidylserine through analyzing Annexin V$^+$/PI$^+$ cells (31 *versus* 38.5%, respectively) (Figure 1c). Bcl-xL is antiapoptotic protein in Bcl-2 family analogous to Bcl-2. Bcl-xL and Bcl-2 suppress apoptosis primarily by the inhibition of cytochrome *c* release. Bcl-xL acts by complexing with and preventing Apaf-1 from activating caspase 9. Bcl-xL and Bcl-2 can inhibit GzmB-mediated caspase-dependent cytolysis, whereas both of them cannot influence human or rat GzmA-induced death.[21,28,29] To verify further the caspase independence of GzmK-induced apoptosis, GzmK was added into HeLa cells transfected to overexpress Bcl-xL or GFP control. Bcl-xL was overexpressed in HeLa cells for 3 days and got high expression probed by anti-HA tag antibody (Ab) (Figure 1b). Overexpression of Bcl-xL

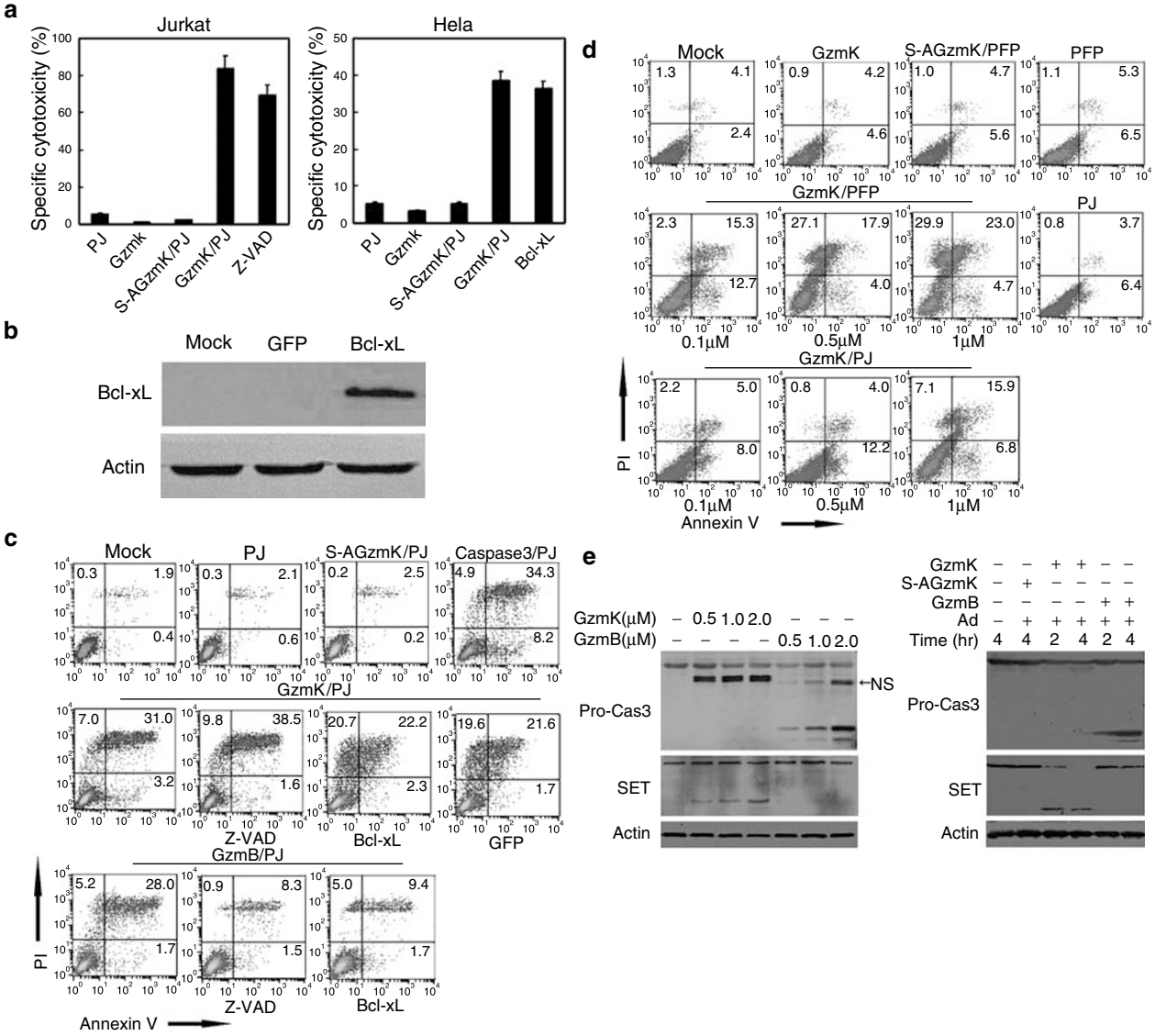

Figure 1 GzmK induces caspase-independent cell death. (**a**) GzmK induces cytotoxicity independently of caspase activation. Jurkat or HeLa cells were treated with GzmK (2 μM), S-AGzmK (2 μM) and/or PJ at 37°C for 4 h. The caspase pan inhibitor Z-VAD-fmk (100 μM) was added to the ^{51}Cr labeled cells 15 min before GzmK loading with PJ. Overexpression of Bcl-xL in HeLa cells did not inhibited GzmK-mediated cytolysis. ^{51}Cr release from Bcl-xL-overexpressed HeLa cells treated with PJ, GzmK alone or S-AGzmK/PJ was comparable to the background level (data not shown). Data are the means of six independent experiments for each cell line. (**b**) Bcl-xL was expressed in HeLa cells after 3 days transfection with pCMV-Bcl-xL-HA vector. Bcl-xL overexpression was probed by anti-HA tag mAb. β-Actin was used as a loading control. (**c**) GzmK loading leads to phosphatidylserine externalization without caspase activation. Target cells were treated with GzmK (2 μM) plus PJ at 37°C for 4 h and stained with Fluos-conjugated Annexin V and PI for analysis by flow cytometry. Cells loading with caspase 3 plus PJ were used as a positive control. A 100 μM portion of ZVAD-fmk treatment or Bcl-xL overexpression did not affect GzmK-induced phosphatidylserine exposure, but significantly inhibited GzmB (2 μM)-mediated death. Data are representative of three separate experiments. (**d**) GzmK can be delivered by PFP leading to death. A total of 2×10^5 Jurkat cells were treated with the indicated concentrations of GzmK in the presence of sublytic PFP (10 nM) or the optimal dose of PJ at 37°C for 4 h and analyzed as above. Similar results were found in HeLa cells (data not shown). The data are representative of at least three separate experiments. (**e**) GzmK does not activate caspase 3. Cell lysates (2×10^5 cell equivalents) treated with different concentrations of GzmK and B as indicated for 2 h were detected for cleavage of procaspase 3 and SET. GzmK cannot process procaspase 3, whereas GzmB can process. SET was probed in the same blot. GzmK cut SET as a positive control, whereas GzmB did not degrade SET. β-Actin was used as negative controls for GzmK or B. The same results were found in 2 μM GzmB or GzmK loaded cells with Ad. GzmK did not activate caspase 3 or ICAD in GzmK-treated cells (data not shown). NS: non-specific band

did not affect GzmK-induced cytolysis markedly as analyzed by ^{51}Cr release or Annexin V plus PI staining assay (Figure 1a, c). However, Bcl-xL overexpression significantly inhibited GzmB-mediated cell death (28 *versus* 9.4%). To further verify caspase independency of GzmK-induced death, we detected procaspase processing and cleavage of caspase substrate ICAD (DFF45) in GzmK-treated lysates or intact cells. Capase activation is a hallmark of caspase-dependent apoptotic pathway. Caspase 3 is a key executioner in the induction of caspase-driven apoptosis. Procaspase 3 is processed at aspartic acid residues by other caspases or by GzmB. Even high concentration of GzmK (2 μM) cannot degrade procas-

pase 3 in GzmK-treated cell lysates as shown in Figure 1e, whereas GzmB cut procaspase to its active form in a dose-dependent manner. The same blot was stripped and reprobed for SET. SET was processed by GzmK, not GzmB. β-Actin was not cleaved by GzmK or B as a loading control. In GzmK (2 μM) loaded HeLa cells, procaspase 3 was not processed by GzmK, which indicates caspase was not activated in GzmK-treated cells. Whereas procaspase 3 was activated by GzmB (2 μM), SET was cut by GzmK, not GzmB. β-Actin was probed as a loading control. GzmK cannot degrade ICAD in GzmK-treated cell lysates or loaded cells (data not shown), whereas ICAD was cut by GzmB in the same blot. Taken together, human GzmK triggers rapid cell death independently of caspase activation.

GzmK initiates apoptotic morphological changes of the nucleus. Perforin delivers Gzms into target cell cytosol to trigger apoptosis by endocytosis. Several studies have shown Ad and bacterial PFP-like streptolysin or listeriolysin can cause endosomal disruption, which substitute for perforin to introduce Gzms into target cell cytosol to initiate apoptosis.[30,31] Direct microinjection of GzmB into target cell cytoplasm results in apoptosis, which suggests the major function of perforin is to deliver Gzms into target cell cytosol. To understand the features of GzmK-induced death, we introduced GzmK into target cells with PJ and visualized nuclear morphological changes using a transmission electron microscopy and a laser scanning confocal microscopy. GzmK can move into the cytosol and the nuclei of target cells within 20 min, and the nuclei show obviously condensed within 2 h (data not shown and Figure 2a). The nuclei appeared shrunken and segmented by 4 h and collapsed within 6 h. The similar results were confirmed by transmission electron microscopy (Figure 2b). PJ and GzmK alone or inactive S-AGzmK plus PJ displayed no distinct features of cell death. Thus, GzmK introduced into target cytosol by PJ induces cytolysis and apoptotic nuclear morphology within hours, which is similar to those observed for GzmA loading with PFP (data not shown and Fan *et al.*[32]).

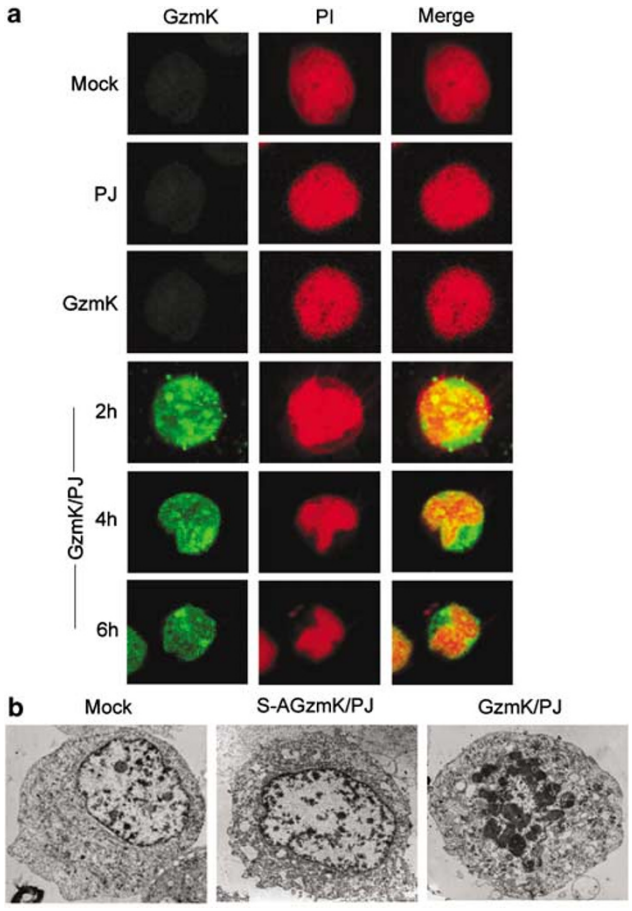

Figure 2 GzmK initiates apoptotic nuclear morphology. (**a**) Kinetic uptake of GzmK and apoptotic nuclear changes. Jurkat cells were treated with GzmK (2 μM) plus PJ at 37°C for the indicated times and fixed for immunostaining. Anti-His-tag mAb was used for probing GzmK, and stained with the secondary Alexa488-conjugated donkey anti-mouse IgG plus PI. GzmK staining green fluorescence was shown at left, PI staining red in the middle, and the merged image at right. (**b**) GzmK loading triggers chromatin condensation and nuclear collapse. HeLa cells were incubated with GzmK or S-AGzmK and/or PJ at 37°C for 4 h. Cells were fixed with 2% glutaraldehyde at 4°C for 1 h, post-fixed with 2% osmium tetroxide, dehydrated and embedded. The ultrathin sections were visualized by JEM-100 CX transmission electron microscopy

GzmK degrades the NAP SET *in vitro* and *in vivo*. The NAP SET was initially identified as a translocated gene in acute undifferentiated leukemia.[33] SET and its homologs bind to the transcriptional coactivators CBP/p300 and the core histones and may serve as a link between transcriptional coactivator and chromatin. We previously demonstrated that GzmA triggers cell death through targeting an ER-associated SET complex, which contains SET and other GzmA substrates the DNA-binding protein high-mobility protein-2 HMG2 and the rate-limiting base-excision repair enzyme apurinic/apyrimidinic endonuclease-1 Ape1.[9] GzmA cleaves SET and abrogates its NAP activity. We next wanted to determine whether the alternate tryptase GzmK degrades SET or not. We found GzmK cut rSET at a very low concentration of 50 nM (Figure 3a). No intact full-length SET was probed at the highest concentration. SET degradation by GzmK was in the similar pattern to GzmA (Figure 3a, b). A 21 kDa cleavage product appeared with the same cleavage site as GzmA.[27] Inactive S-AGzmK had no proteolytic action. It indicates the degradation needs enzymatic activity of GzmK. rpp32 was not cleaved as a good negative control. rSET was hydrolyzed by GzmK after 30 min (Figure 3a). Full length of rSET was undetectable after 1 h. By 3 h, the cleavage product of rSET was almost disappeared, whereas inactive S-AGzmK was without effect even after 4 h. GzmK can directly cleave rSET. We wanted to look at whether GzmK hydrolyzes native SET in cell lysates. A 0.5 μM portion of GzmK began to process native SET to produce a cleaved band in a dose-dependent manner (Figure 3b). The same blot was stripped and reprobed for pp32. pp32 was unchanged as a loading control. Native SET was degraded within 30 min and full length of SET was almost cleaved completely within 2 h (Figure 3b). pp32 was unchangeable at all time points.

To further investigate whether SET cleavage is physiologically relevant, we visualized SET degradation in GzmK loaded cells (Figure 3c). Cytosolic SET cleavage occurred after 2 h in

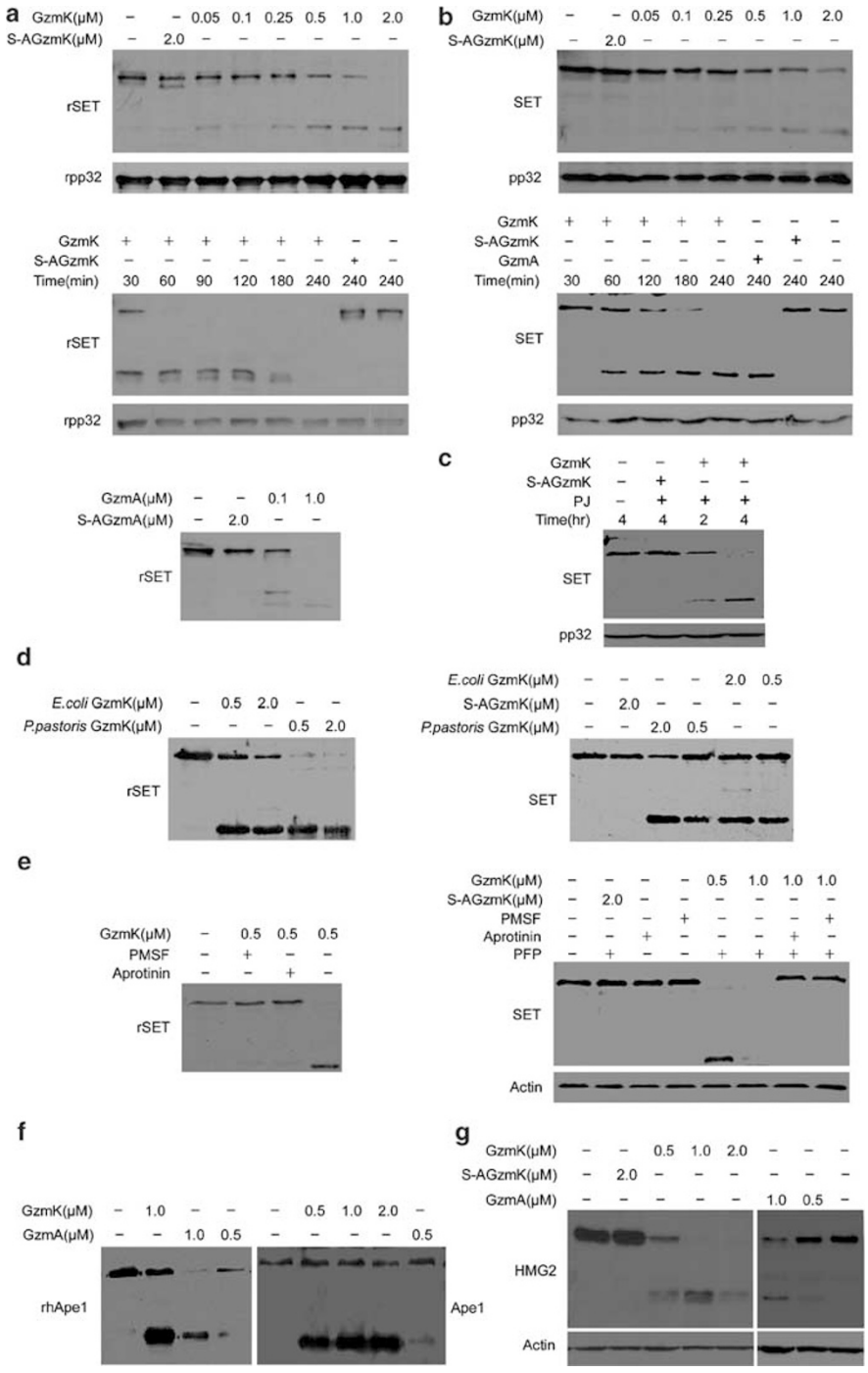

Figure 3 GzmK cleaves SET and other GzmA substrates of SET complex. (**a**) rSET was degraded by GzmK in a dose- and time-dependent manner. A 1 μM portion of rSET was incubated at 37°C for the indicated times with different concentrations of GzmK or S-AGzmK. Reactions were stopped by adding 5 $\times$ SDS loading buffer and analyzed by immunoblotting with anti-SET Ab. GzmK did not cleave rpp32 as a negative control. The SET cleavage pattern by GzmA was similar to that by GzmK. (**b**) GzmK cleaves native SET. Jurkat cell lysates were treated with GzmK at 37°C in the indicated concentrations and times. SET and pp32 were probed as above. pp32 was unchanged as a good loading control. Similar results were obtained in HeLa cell lysates (data not shown). (**c**) GzmK cleaves SET in cells. Jurkat cells were treated for the indicated times at 37°C with GzmK (2 μM) or S-AGzmK (2 μM) plus PJ. The whole-cell lysates were analyzed by immunoblotting using anti-SET Ab and pp32 mAb. (**d**) GzmK expressed from *E. coli* and *P. pastoris* shares similar enzymatic activity. A 1.0 μM portion of rSET and cell lysates (2×10^5 cell equivalents) were treated with the two forms of rGzmK and probed for SET by immunoblot. (**e**) SET cleavage by GzmK can be blocked by a trypsin inhibitor aprotinin or a broad-spectrum serine protease inhibitor PMSF. A 0.5 μM portion of GzmK pretreated with aprotinin (0.015 mM) or PMSF (2 mM) for 15 min was incubated with 0.5 μM rSET at 37°C for 1 h and probed with anti-SET Ab. A total of 2×10^5 Jurkat cells were treated with the indicated concentrations of active GzmK and aprotinin or PMSF pretreated GzmK (1 μM) in the presence of sublytic PFP (10 nM) at 37°C for 4 h and analyzed as above. (**f**) GzmK hydrolytes Ape1 with the same cleavage pattern to GzmA. A 1 μM portion of rhApe1 and cell lysates (2×10^5 cell equivalents) were treated by GzmK and A and probed with Ape1 Ab. (**g**) GzmK degrades HMG2 similar to GzmA. Cell lysates (2×10^5 cell equivalents) were incubated with different dose of GzmK and A as indicated at 37°C for 2 h and probed with HMG2 Ab. Similar results were found for rHMG2 degradation by GzmK and A (data not shown)

2 μM GzmK loading with PJ. SET degradation was increased during the process of undergoing death. S-AGzmK plus PJ or Mock-treated cells did not cause SET cleavage. pp32 was unchanged at all time course as a good loading control. SET cleavage requires enzymatic activity of GzmK. The GzmK concentration needed to degrade SET in cells is comparable to that needed to induce cell death and nuclear morphology as described above. Therefore, SET is a direct physiological substrate of GzmK *in vivo*.

To compare the enzymatic activity of glycosylated or non-glycosylated GzmK, cleavage of recombinant and native SET was treated by rGzmK from *E. coli* and *Pichia pastoris*. We expressed hGzmK in the methylotrophic yeast *P. pastoris* and purified with affinity chromatography. As a eucaryote, *P. pastoris* can carry out protein processing, protein folding and post-translational modification such as glycosylation. We found GzmK from *P. pastoris* had higher molecular weight than that from *E. coli* resolving on denatured SDS-PAGE gels (data not shown). Both forms of rGzmK degraded recombinant and native SET with the same cleavage pattern (Figure 3d). rGzmK from *P. pastoris* had a little bit higher hydrolytic activity than that from *E. coli*. Whether *in vivo* GzmK requires being glycosylated remains to be further investigated. To verify the specific enzymatic activity of GzmK, 0.5 μM GzmK pretreated with a trypsin inhibitor aprotinin (0.015 mM) or a broad-spectrum serine protease inhibitor phenylmethylsulfonyl fluoride (PMSF) (2 mM) was incubated with 0.5 μM rSET at 37°C for 1 h. Aprotinin- or PMSF-pretreated GzmK did not degrade its substrate rSET (Figure 3e). Enzymatic GzmK degraded all the full length of SET to its cleaved form within 1 h. We further confirmed this observation by loading GzmK into target cells in the presence of PFP. A total of 2×10^5 Jurkat cells were treated with different concentrations of active GzmK and aprotinin- or PMSF-pretreated GzmK (1 μM) in the presence of sublytic PFP (10 nM) at 37°C for 4 h. A 0.5 μM portion of enzymatic GzmK degraded all the full length of SET to its cleaved form (Figure 3e). SET was completely degraded by 1 μM GzmK, whereas aprotinin- or PMSF-pretreated GzmK did not cleave SET. Aprotinin or PMSF alone and inactive S-AGzmK plus PFP had no effect. The same blot was stripped and probed by β-actin as a loading control. β-Actin was unchangeable at all samples. Taken together SET cleavage is induced by the enzymatic GzmK. These results are consistent with Wilharm *et al*.[25] observations.

rGzmK from *E. coli* degraded Ape1 in its recombinant and native forms in a dose-dependent manner with the same cleavage patterns as GzmA (Figure 3f). Similar results were found for HMG2 cleavage in cell lysates or recombinant form by GzmK and A (Figure 3g and data not shown). β-Actin was probed as a negative control. It indicates that GzmK shares partial redundancy for some physiological substrates to GzmA. Whether GzmK induces cytolysis through targeting the same SET complex as GzmA remains to be further study.

Cleavage of SET by GzmK abolishes its NAP activity. SET has been shown to bind histones and have NAP activity.[24,27] Topoisomerase-relaxed plasmid was incubated with purified core histones in the presence of different concentrations of rSET. rSET facilitated plasmid DNA assembly in a dose-dependent manner (Figure 4a). The NAP activity of SET is ATP and sequence independent, similar to our previous findings.[24] We previously showed that cleavage of recombinant and native SET by GzmA abrogates the NAP activity of SET with dose dependence. Thus, we wanted to detect whether SET degradation by GzmK abolishes its NAP activity. Pretreatment of rSET with GzmK disabled the NAP activity of SET with a dose-dependent manner (Figure 4b). A 0.5 μM portion of GzmK treatment did not inhibit the NAP activity, whereas 1 μM GzmK completely abrogated the NAP function of SET. GzmK alone did not have any assembly activity to plasmid DNA. The acidic tail of full-length SET is responsible for its NAP function. N- and C-terminal fragments degraded by GzmA have not any NAP activity.[27] SET degradation by GzmK was in the similar pattern to GzmA and also disrupted the NAP action of SET.

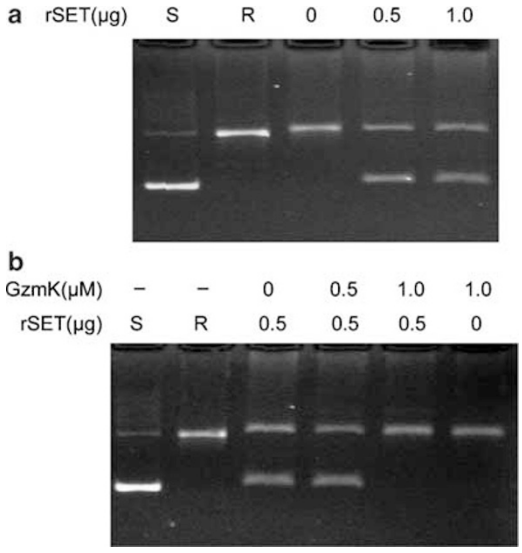

Figure 4 SET cleavage by GzmK disrupts its NAP activity. (**a**) rSET has NAP activity. rSET was preincubated with core histones before adding topoisomerase-relaxed plasmid pBR322 (R). After 1 h at 37°C, the reaction mixture was deproteinized and analyzed by agarose gel electrophoresis. rSET assembled plasmid DNA along with core histones to generate supercoiled plasmid (S). (**b**) GzmK preincubation with rSET abolishes its NAP activity. A 0.5 μg portion of rSET was pretreated with the indicated amounts of GzmK at 37°C for 2 h before mixing with core histones and relaxed plasmid. GzmK without SET did not cause plasmid assembly

GzmK triggers single-stranded DNA nicks. We previously showed that GzmA induces single-stranded DNA nicking, not double-stranded DNA fragmentation.[24,28] Rat GzmK was reported to cause slow acting DNA fragmentation after 20 h.[20] It is unknown about how human GzmK targets chromosomal DNA to trigger death. The DNA polymerase Klenow labeling was used to assess DNA strand breaks as described.[24] GzmK (2 μM) loading with PJ led to increased ^{32}P-dATP incorporation. ^{32}P-dATP incorporation of cells treated with GzmA plus PJ were as a positive control (Figure 5a). S-AGzmK alone or S-AGzmK plus PJ just got comparable background incorporation to Mock-treated cells. These results were confirmed by denaturing alkaline agarose

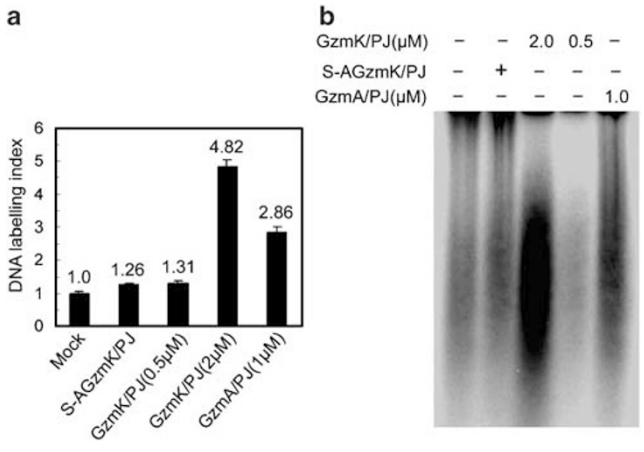

Figure 5 GzmK initiates single-stranded DNA nicks. (**a**) Jurkat nuclei were isolated from the cells loaded with GzmK (1 μM) or GzmA (1 μM) plus PJ at 37°C for 4 h and radiolabeled through Klenow DNA polymerase. The radioactivity counts of ^{32}P-dATP Klenow incorporation were determined by Storm and analyzed with ImageQuant 5.2 program (Pharmacia). The specific labeling index was normalized to the level of labeling detected in Mock-treated cells. (**b**) The DNA nicks were verified by the denaturing alkaline gel electrophoresis

gel electrophoresis (Figure 5b). ^{32}P-dATP incorporation derived from 1 μM GzmK plus PJ loading was comparable to that of the same molar GzmA plus PJ (data not shown). The oligonucleosomal DNA fragmentation was not visualized in GzmK loaded cells as treated above by agarose gel electrophoresis (data not shown). The oligonucleosomal DNA fragmentation induced by GzmK was not visualized by agarose gel electrophoresis (data not shown). Taken together, human GzmK induces single-stranded DNA nicks as human GzmA.

GzmK unleashes the GAAD NM23H1 to translocate into the nucleus for nicking DNA. We previously demonstrated the GAAD is NM23H1, which binds to its inhibitor (IGAAD) SET and is predominantly cytoplasmic and associated with the ER in the SET complex.[24] The DNase activity of NM23H1 was activated via degradation of its inhibitor SET. GzmA can cleave SET to release NM23H1 endonuclease action and initiate NM23H1 translocation into the nucleus to nick DNA. As SET is a substrate of GzmK, we next determined whether human GzmK causes NM23H1 nuclear translocation to damage DNA. HeLa cells were lysed and fractionated at different time points post GzmK loading with PJ. NM23H1 and SET were visualized by immunoblotting. NM23H1 and SET were in the cytoplasmic fraction in untreated cells or cells treated with GzmK or PJ alone. Within 10 min after GzmK loading plus PJ, NM23H1 and SET began to move into the nucleus (Figure 6a). By 1 h, NM23H1 and SET mostly appeared in the nuclear fraction. The cleavage product of SET was only detected in the nucleus. β-Actin and histone H3 were probed to validate the complete separation of the cytoplasmic and the nuclear fraction. The cytosolic protein β-actin only existed in the cytoplasmic fraction and the nuclear protein histone H3 merely appeared in the nuclear fraction. These results were further confirmed by confocal microscopy. NM23H1 and SET were primarily perinuclear in untreated HeLa cells or cells treated with GzmK or PJ alone (Figure 6b). In contrast, NM23H1 mostly moved into the nucleus within 30 min in cells treated with GzmK plus PJ. SET translocated into the nucleus in a similar pattern with NM23H1. It indicates SET cleavage by GzmK triggers NM23H1 activation and translocation to nick chromosomal DNA analogous to GzmA.

Discussion

Although human GzmK has been cloned for near two decades, it is unclear about its action in granule-mediated cytolysis. Rat GzmK, also known as fragmentin 3, was originally identified as the third proteolytic inducer of DNA fragmentation in PFP-treated YAC-1 cells apart from GzmA and B.[20] GzmK is a tryptase and preferentially hydrolyze the Z-Lys-SBzl and Z-Arg-SBzl substrates, similar to human GzmA. Rat GzmK induced DNA fragmentation after 20 h and considered as a slow acting Gzm, whereas GzmB causes DNA fragmentation within 2 h. The same group also showed that rat GzmK loading with PFP did not cause any apoptotic nuclear morphological changes resembled as untreated control cells.[21] We expressed human active GzmK and investigated its role in targeting cell death. We utilized PJ to load GzmK, A or B into target cells that led to similar apoptotic features and cleavage of their substrates as perforin- or Ad-delivered GzmK, A or B (data not shown). PJ can imitate PFP for delivering Gzms into target cells *in vitro*. However, the delivery efficiency of Gzms by perforin is more efficient than that by PJ. This may be because the cationic lipid-based PJ-combined Gzms complex needs to attach negatively charged cell surfaces and enters the cytoplasm either by directly fusing with the plasma membrane or by endocytosis and subsequent fusion with the endosome, releasing the captured Gzms into the cytoplasm, which maybe takes longer time to release Gzms than that delivered by perforin. Whereas perforin delivers Gzms into the cytosol by endocytosis through its polymerization.[22] The different delivery efficiency by PFP and PJ needs to be further investigated. We first demonstrated here human GzmK induces rapid cell death with typical chromatin condensation and apoptotic nuclear morphological features. The DNA damage initiated by human GzmK is single-stranded DNA nicks, not double-stranded DNA fragmentation.

Human GzmK induces the single-stranded DNA nicks analogous to human GzmA, which is not labeled by the terminal deoxynucleotidyl transferase (TdT). Moreover, the nicked DNA fragments are large and fail to release into culture supernatants, which is undetectable by ^{125}I-UdR labeling assay that was used by the previous report.[20] So the nicked DNA cannot be visualized via conventional apoptotic assays using non-denaturing agarose gels or TdT labeling. However, DNA nicks can be detected through Klenow polymerase labeling assay as we described previously.[24] We found human GzmK triggers DNA nicks within hours. GzmK does not induce oligonucleosomal DNA fragmentation (data not shown). GzmK induces nuclear morphological features within hours like GzmA analyzed by several apoptotic assays as described above. These data indicate human GzmK is a fast-acting protease similar to human GzmA.

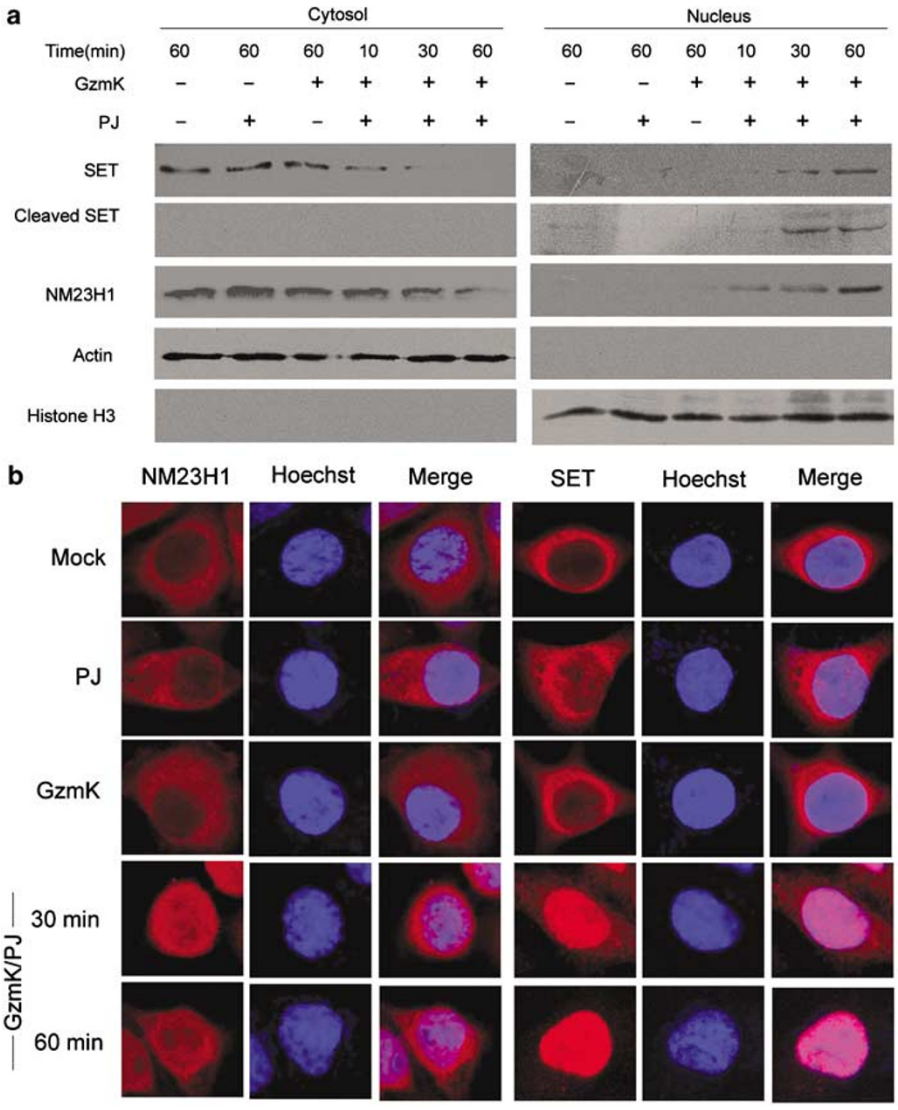

Figure 6 GzmK triggers the DNase NM23H1 translocation from the cytoplasm to the nucleus. (**a**) GzmK and PJ treatment of HeLa cells induces translocation of NM23H1 and its inhibitor SET. NM23H1 and SET were predominantly in the cytoplasm from the untreated cells. A progressive decrease in the cytosol and corresponding increase in the nucleus of NM23H1 and SET appeared in the process of the GzmK (1 μM) and PJ treatment. SET was degraded in the nucleus. GzmK or PJ alone was without effect on the translocation of NM23H1 and SET. The cytosolic protein β-actin and the nuclear protein histone H3 were probed to verify the complete separation of the cytoplasmic and nuclear fractions. (**b**) The rapid nuclear translocation of NM23H1 and SET were confirmed via confocal microscopy. The DNase NM23H1 and its inhibitor SET translocated quickly to the nucleus within 30 min after GzmK (1 μM) loading with PJ. NM23H1 and SET staining red fluorescence was shown at left, Hoechst staining blue in the middle and the merged image at right. The data represent one out of three separate experiments

We previously identified the GAAD is NM23H1. The NAP SET is its inhibitor (IGAAD).[24] GzmA activates the DNase activity by degrading SET, disrupting its binding to NM23H1 and unleashing it from inhibition. This mechanism is reminiscent of the activation of CAD by caspase or GzmB cleavage of ICAD.[34] In both pathways, the endonuclease activity is sequestered in the cytosol bound to its inhibitor of normal cells. Upon cell death, the uninhibited DNase translocates to the nucleus. GzmK can cleave the IGAAD SET and release GAAD NM23H1, which rapidly translocates into the target nucleus to nick chromosomal DNA. A recent study showed that mitochondrial damage is key to the SET complex nuclear translocation and GzmA induction of apoptosis.[12] Furthermore, SET complex proteins move synchronously into the nucleus in response to different oxidative stresses. GzmA loading triggers rapid ROS generation, which leads to fast SET complex protein translocation. Nevertheless, superoxide scavengers inhibit ROS generation and block SET complex translocation. These results indicate ROS causes SET complex protein translocation into the nucleus. One report showed that rat GzmK destroys mitochondrial membrane potential and induces ROS production.[21] How human GzmK targets mitochondria requires to be elucidated.

Cytotoxic granules contain multiple Gzms, which hold different serine protease activities. Among human Gzms, GzmK and A share the same tryptase activity.[35] They are closely linked together on the same chromosome. GzmA-deficient mice do not alter GzmK gene and its expression and still exist tryptase activity.[36] GzmK might be responsible for the residual tryptase activity. GzmA-knockout mice have normal growth, development, and normal lymphocyte development, activation and proliferation. GzmA-deficient mice just appear slight defect in some certain virus infection.[14] GzmK may rescue the cytotoxicity in GzmA-deficient killer lymphocytes. However, it is unknown about whether these two tryptases are redundant or not. GzmA is the most abundant Gzm in cytotoxic granules of humans and mice, which exerts its function with a dimer form. GzmA induces a caspase-independent death pathway with chromatin condensation, nuclear morphological changes, mitochondrial dysfunction and single-stranded DNA damage.[9] The molecular mechanism of GzmA-mediated cell death is through targeting a 270–420 kDa ER-associated SET complex, which includes three GzmA sustrates SET, HMG2 and Ape1.[24,32,37] GzmA cuts these three substrates and abolishes their normal functions to trigger apoptosis of target cells. GzmK is less abundant than GzmA in activated human killer lymphocytes. But GzmK has higher enzymatic tryptase activity.[19] Unlike GzmA, the active form of GzmK is a monomeric structure. The crystal structure of GzmK zymogen has recently been determined.[38] Its substrate specificity has just been analyzed through the chemical functional probes.[35] GzmK and A share similar crossreactivity at P1, but distinct specificities at P4–P2. It is unknown about the specific physiological substrates of GzmK in target cells. We first showed here that GzmK can cleave GzmA substrates of the SET complex proteins, SET, HMG2 and Ape1 in the same proteolytic patterns as GzmA. It indicates GzmK shares partial redundancy to GzmA. A study showed that cytotoxic lymphocytes from mice lacking either GzmA, B or both exhibit a relatively normal ability to lyse target cells.[39] This indicates other Gzms rescue the killing activity to the target. It suggests multiple Gzms might have redundant roles or partial redundancy and provide back-up mechanisms for restoring functional defects of Gzms in killer cells. Whether GzmK makes GzmA totally redundant remains to be further investigated.

Materials and Methods

Cell lines, Abs and reagents. Cells were grown in RPMI 1640 (Jurkat) and DMEM medium (HeLa) supplemented with 10% fetal calf serum, 50 mM β-mercaptoethanol, 100 U/ml penicillin and streptomycin. Commercial Abs were rabit antisera against HMG2 (PharMingen), NM23H1 (Santa Cruz), Ape1 (Santa Cruz), caspase 3 (BD PharMingen), mouse mAb against His-tag (Sigma Aldrich), β-actin (Sigma Aldrich), histone H3 (Cell Signaling), HRP-conjugated sheep anti-mouse IgG, HRP-conjugated sheep anti-rabbit IgG (Santa Cruz) and Alexa488-conjugated donkey anti-mouse IgG (Molecular Probes). Rabbit SET antisera and mouse pp32 mAb were generated as described.[24] Lipofectamine™ 2000 was from Invitrogen and Pro-Ject™ protein transfection reagent kit was from Pierce Biotechnology. Annexin V-fluorescein isothiocyanate (FITC) was from BD Pharmingen, ProLong and Antifade kit was from Molecular Probes. Perforin (PFP) was a kind gift of Dr. Trapani's Lab (Research Division, Peter MacCallum Cancer Centre, Australia).

Production of active and inactive mutated GzmK by *E. coli* and *P. pastoris*. The full-length cDNA of human GzmK was PCR amplified from GzmK cDNA clone (RZPD Deutsches Ressourcenzentrum). Primers were constructed from the human GzmK sequence to contain an enterokinase site 5′ of the predicted first amino acid of the active enzyme and *Nco*I and *Xho*I restriction sites. The PCR product was directly ligated into pET26b (Novagen). The subcloned GzmK sequence was verified by dideoxynucleotide sequencing. GzmK expression plasmid was transfected into BL21-DE3 (Novagen) and induced with 1 mM isopropyl β-dathiogalactoside. Recombinant GzmK was purified by a Novagen nickel column and desalted into enterokinse buffer (20 mM Tris-HCl/50 mM NaCl/2 mM $CaCl_2$) and digested with 4 U of enterokinase at 25°C for 16 h and repurified by a nickel column. GzmK concentration was determined by BCA assay. GzmK catalytic site serine 214 was mutated to alanine by PCR mutagenesis. The mutated S-AGzmK sequence was subcloned to pET26b and confirmed by DNA sequencing. S-AGzmK was expressed and purified as above with cathepsin C digestion.[25] For GzmK expression in *P. pastoris*, the cDNA sequences encoding human GzmK and its inactive mutant (S214A) were PCR amplified and subcloned into the yeast expression vector pPICZαA immediately following the Kex2 signal cleavage site of the *Saccharomyces cerevisiae* α-factor secretion signal (Invitrogen). The construction was linearized with *Sac*I and transformed into the X33 strain of *P. pastoris* according to the manufacturer's instruction. Multicopy recombinants were isolated with increasing concentrations of Zeocin (Invitrogen). After 72 h induction with 1% methanol, the supernatant was harvested and loaded onto the QuiStand benchtop system (Amersham Biosciences) for concentration and buffer exchange. Recombinant GzmK was purified using affinity chromatography. The concentration of recombinant GzmK was determined by BCA assay as above. The hydrolytic activity of GzmK was performed using N^{α}-benzyloxycarbonyl-L-lysine-thiobenzyl ester (Z-Lys-SBzl) as described.[25]

Loading GzmK with PJ or Ad or perforin. Cells were washed three times in HBSS and resuspended in loading buffer (HBSS with 0.5 mg BSA/ml, 1 mM $CaCl_2$ and 1 mM $MgCl_2$ for PJ loading; and HBSS with 10 mM HEPES buffer, pH 7.2, 1 mM $CaCl_2$ and 0.02% BSA perforin loading). HeLa cells or Jurkat cells (2×10^5) in 50 μl of loading buffer were incubated at 37°C for the indicated times with different concentrations of GzmK, S-AGzmK, caspase 3 and/or an optimal dose of PJ or Ad or sublytic perforin. Cells were incubated for an additional 15 min in 1 mM PMSF before being lysed for immunoblotting. Loading GzmK with perforin was performed as described previously.[15,40] Briefly, a sublytic dose was first titrated with recombinant perforin. Then the sublytic dose of perforin was used in combination with GzmK or S-AGzmK at each assay.

Cytotoxicity assay. Target cells were labeled with ^{51}Cr at 37°C for 1 h. After completely washing, 1×10^4 target cells were incubated with GzmK, S-AGzmK and/or PJ at 37°C for 4 h. ^{51}Cr release of supernatant from each tube was carefully removed to a disposable tube and counted on the 1450 MicroBeta counter (Pharmacia). For caspase dependence assay, cells were pretreated with 100 μM ZVAD-fmk before GzmK loading with PJ. Specific release was calculated as ((sample release−spontaneous release)/(total release−spontaneous release)) × 100.

Flow cytometry analysis. FITC-conjugated Annexin V was used to evaluate phosphatidylserine externalization. Target cells treated with S-AGzmK, GzmK, GzmB, caspase 3 and PJ were stained with Annexin V-Fluos and PI and analyzed by flow cytometry using a FACSCalibur (BD Biosciences).

Electron microscopy. HeLa cells (5×10^5) were treated with GzmK plus PJ at 37°C for 4 h. Cells were washed twice and fixed with 2% glutaraldehyde at 4°C for 1 h and post-fixed with 2% osmium tetroxide. Cells were dehydrated with sequential washes in 50, 70, 80, 90 and 100% ethanol, and then embedded in Spurrs resin. Ultrathin sections were obtained, mounted in copper grids, counterstained with uranyl acetate and lead citrate, and examined in a JEM-100 CX transmission electron microscopy. Images were photographed and scanned by Eversmart Jazz + program (Scitex).

Laser scanning confocal microscopy. Jurkat cells were treated with GzmK plus PJ for the indicated times, and then plated on polyLys-coated slides and incubated at RT for 1 h with 5 μg/ml anti-His-tag mAb, 50 μg/ml donkey serum and 100 μg/ml RNase I. After washing twice with PBS, the cells were stained with Alexa488-conjugated donkey anti-mouse IgG, and soaked for 5 min in PBS containing 0.1 μg/ml PI. The slides were mounted and observed using laser scanning confocal microscopy (Olympus FV500 microscope). For translocation assay, HeLa cells (2×10^4) grown overnight on Felcon culture slides (Molecular

Probes) were washed twice with PBS and treated with GzmK plus PJ at 37°C for the indicated times. After an additional wash with 1 mM PMSF, cells were fixed with 4% paraformaldehyde for 20 min at RT and permeabilized with 1% Triton X-100 for another 20 min, then stained with anti-NM23H1 or anti-SET polyclonal Ab and then with the secondary Ab Alexa594-conjugated donkey anti-rabbit IgG. Cells were visualized as above.

SET cleavage and GzmK inhibition assay. rSET or cell lysates (2×10^5 cell equivalents) were incubated at 37°C for the indicated times with different concentrations of GzmK, S-AGzmK or GzmA in 20 μl cleavage buffer (50 mM Tris-HCl pH 7.5, 1 mM $CaCl_2$, 1 mM $MgCl_2$). The reaction products were boiled in 5 $\times$ SDS loading buffer before SDS-PAGE. For *in vivo* cleavage assay, cells loaded with GzmK and PJ were lysed with 0.5% NP-40 lysis buffer. The lysates were probed by immunoblotting. GzmK inhibition assays were performed as described previously.[25] A 0.015 mM portion of aprotinin or 2 mM PMSF was used in each experiment.

Klenow incorporation assay. DNA polymerase Klenow fragment was used to label DNA nicks as described.[24] Briefly, 4 h treatment with GzmK plus PJ, cells were lysed in an equal volume of 0.5% NP-40 lysis buffer and incubated with 5 U Klenow and 10 μCi ^{32}P-dATP at 37°C for 1 h. The radiolabeled nuclei were washed completely and analyzed for DNA labeling index. The radioactivity counts were determined directly with Storm program (Pharmacia). All data for each specific labeling were normalized to the level of labeling detected in Mock-treated cells. Alkaline agarose gel electrophoresis was used to verify single-stranded DNA nicks as described.[24]

NAP activity assay. Nucleosome assembly assay was carried out as described previously.[26] Briefly, 1 μg topoisomerase I relaxed pBR322 plasmid DNA was treated with the indicated doses of rSET plus 1 μg purified core histones in the assay buffer (150 mM NaCl, 1 mM EDTA, 100 μg/ml BSA and 10 mM Tris-HCl, pH 8.0). rSET was pretreated with the indicated concentrations of GzmK or Mock treated at 37°C for 2 h before incubation with the core histones. Samples were electrophoresed using 1.2% agarose gels and visualized by ErBr staining.

Overexpression of Bcl-xL. HeLa cells were transfectd with pCMV-Bcl-xL or pCMV-GFP plasmid in the presence of Lipofectamine™ 2000 according to the manufacturer's introduction. Bcl-xL expression was detected by anti-HA tag Ab by immunoblotting. For cytotoxicity assay, cells were collected 3 days after transfection.

Acknowledgements. We thank W Xu, Y Chen, C Liu, Y Teng and Y Xu for technical support; Dr. J Trapani for providing the recombinant mouse perforin; Dr. C Weng for providing Bcl-xL plasmid. This work was supported by The Hundred Talents Program of CAS to ZF and grants from the National Natural Science Foundation of China Program (30500448 and 30470365) and the Outstanding Youth Grant (30525005). Special Grants for President Scholarship and Innovation Study of CAS for outstanding graduate students, China Postdoctoral Science Foundation and KC Wong Education Foundation (Hong Kong) to TZ.

1. Russell JH, Ley TJ. Lymphocyte-mediated cytotoxicity. *Annu Rev Immunol* 2002; **20**: 323–370.
2. Fan Z, Zhang Q. Molecular mechanisms of lymphocyte-mediated cytotoxicity. *Cell Mol Immunol* 2005; **2**: 259–264.
3. Stinchcombe JC, Bossi G, Booth S, Griffiths GM. The immunological synapse of CTL contains a secretory domain and membrane bridges. *Immunity* 2001; **15**: 751–761.
4. Hayes MP, Berrebi GA, Henkart PA. Induction of target cell DNA release by the cytotoxic T lymphocyte granule protease granzyme A. *J Exp Med* 1989; **170**: 933–946.
5. Podack ER, Young JD, Cohn ZA. Isolation and biochemical and functional characterization of perforin 1 from cytolytic T-cell granules. *Proc Natl Acad Sci USA* 1985; **82**: 8629–8633.
6. Pasternack MS, Eisen HN. A novel serine esterase expressed by cytotoxic T lymphocytes. *Nature* 1985; **314**: 743–745.
7. Barry M, Bleackley RC. Cytotoxic T lymphocytes: all roads lead to death. *Nat Rev Immunol* 2002; **2**: 401–409.
8. Grossman WJ, Revell PA, Lu ZH, Johnson H, Bredemeyer AJ, Ley TJ. The orphan granzymes of humans and mice. *Curr Opin Immunol* 2003; **15**: 544–552.
9. Lieberman J, Fan Z. Nuclear war: the granzyme A-bomb. *Curr Opin Immunol* 2003; **15**: 553–559.
10. Trapani JA, Sutton VR. Granzyme B: pro-apoptotic, antiviral and antitumor functions. *Curr Opin Immunol* 2003; **15**: 533–543.
11. Lieberman J. The ABCs of granule-mediated cytotoxicity: new weapons in the arsenal. *Nat Rev Immunol* 2003; **3**: 361–370.
12. Martinvalet D, Zhu P, Lieberman J. Granzyme A induces caspase-independent mitochondrial damage, a required first step for apoptosis. *Immunity* 2005; **22**: 355–370.
13. Heusel JW, Wesselschmidt RL, Shresta S, Russell JH, Ley TJ. Cytotoxic lymphocytes require granzyme B for the rapid induction of DNA fragmentation and apoptosis in allogeneic target cells. *Cell* 1994; **76**: 977–987.
14. Ebnet K, Hausmann M, Lehmann-Grube F, Mullbacher A, Kopf M, Lamers M *et al.* Granzyme A-deficient mice retain potent cell-mediated cytotoxicity. *EMBO J* 1995; **14**: 4230–4239.
15. Kelly JM, Waterhouse NJ, Cretney E, Browne KA, Ellis S, Trapani JA *et al.* Granzyme M mediates a novel form of perforin-dependent cell death. *J Biol Chem* 2004; **279**: 22236–22242.
16. Johnson H, Scorrano L, Korsmeyer SJ, Ley TJ. Cell death induced by granzyme C. *Blood* 2003; **101**: 3093–3101.
17. Carter CR, Sayers TJ, Wiltrout RH, Turcovski-Corrales SM, Taub DD. Generation of antigenic peptides by lymphocyte granule serine proteases (granzymes). *Cell Immunol* 1996; **172**: 235–245.
18. Davis JE, Smyth MJ, Trapani JA. Granzyme A and B-deficient killer lymphocytes are defective in eliciting DNA fragmentation but retain potent *in vivo* anti-tumor capacity. *Eur J Immunol* 2001; **31**: 39–47.
19. Hameed A, Lowrey DM, Lichtenheld M, Podack ER. Characterization of three serine esterases isolated from human IL-2 activated killer cells. *J Immunol* 1988; **141**: 3142–3147.
20. Shi L, Kam CM, Powers JC, Aebersold R, Greenberg AH. Purification of three cytotoxic lymphocyte granule serine proteases that induce apoptosis through distinct substrate and target cell interactions. *J Exp Med* 1992; **176**: 1521–1529.
21. MacDonald G, Shi L, Vande Velde C, Lieberman J, Greenberg AH. Mitochondria-dependent and -independent regulation of granzyme B-induced apoptosis. *J Exp Med* 1999; **189**: 131–144.
22. Keefe D, Shi L, Feske S, Massol R, Navarro F, Kirchhausen T *et al.* Perforin triggers a plasma membrane-repair response that facilitates CTL induction of apoptosis. *Immunity* 2005; **23**: 249–262.
23. Zelphati O, Szoka Jr FC. Mechanism of oligonucleotide release from cationic liposomes. *Proc Natl Acad Sci USA* 1996; **93**: 11493–11498.
24. Fan Z, Beresford PJ, Oh DY, Zhang D, Lieberman J. Tumor suppressor NM23-H1 is a granzyme A-activated DNase during CTL-mediated apoptosis, and the nucleosome assembly protein SET is its inhibitor. *Cell* 2003; **112**: 659–672.
25. Wilharm E, Parry MA, Friebel R, Tschesche H, Matschiner G, Sommerhoff CP *et al.* Generation of catalytically active granzyme K from *Escherichia coli* inclusion bodies and identification of efficient granzyme K inhibitors in human plasma. *J Biol Chem* 1999; **274**: 27331–27337.
26. Beresford PJ, Kam CM, Powers JC, Lieberman J. Recombinant human granzyme A binds to two putative HLA-associated proteins and cleaves one of them. *Proc Natl Acad Sci USA* 1997; **94**: 9285–9290.
27. Beresford PJ, Zhang D, Oh DY, Fan Z, Greer EL, Russo ML *et al.* Granzyme A activates an endoplasmic reticulum-associated caspase-independent nuclease to induce single-stranded DNA nicks. *J Biol Chem* 2001; **276**: 43285–43293.
28. Beresford PJ, Xia Z, Greenberg AH, Lieberman J. Granzyme A loading induces rapid cytolysis and a novel form of DNA damage independently of caspase activation. *Immunity* 1999; **10**: 585–594.
29. Sutton VR, Vaux DL, Trapani JA. Bcl-2 prevents apoptosis induced by perforin and granzyme B, but not that mediated by whole cytotoxic lymphocytes. *J Immunol* 1997; **158**: 5783–5790.
30. Pinkoski MJ, Hobman M, Heibein JA, Tomaselli K, Li F, Seth P *et al.* Entry and trafficking of granzyme B in target cells during granzyme B-perforin-mediated apoptosis. *Blood* 1998; **92**: 1044–1054.
31. Froelich CJ, Orth K, Turbov J, Seth P, Gottlieb R, Babior B *et al.* New paradigm for lymphocyte granule-mediated cytotoxicity. Target cells bind and internalize granzyme B, but an endosomolytic agent is necessary for cytosolic delivery and subsequent apoptosis. *J Biol Chem* 1996; **271**: 29073–29079.
32. Fan Z, Beresford PJ, Zhang D, Xu Z, Novina CD, Yoshida A *et al.* Cleaving the oxidative repair protein Ape1 enhances cell death mediated by granzyme A. *Nat Immunol* 2003; **4**: 145–153.
33. Von Lindern M, van Baal S, Wiegant J, Raap A, Hagemeijer A, Grosveld G. Can, a putative oncogene associated with myeloid leukemogenesis, may be activated by fusion of its 3′ half to different genes: characterization of the set gene. *Mol Cell Biol* 1992; **12**: 3346–3355.
34. Liu X, Zou H, Slaughter C, Wang X. DFF, a heterodimeric protein that functions downstream of caspase-3 to trigger DNA fragmentation during apoptosis. *Cell* 1997; **89**: 175–184.
35. Mahrus S, Craik CS. Selective chemical functional probes of granzymes a and B reveal granzyme B is a major effector of natural killer cell-mediated lysis of target cells. *Chem Biol* 2005; **12**: 567–577.
36. Shresta S, Goda P, Wesselschmidt R, Ley TJ. Residual cytotoxicity and granzyme K expression in granzyme A-deficient cytotoxic lymphocytes. *J Biol Chem* 1997; **272**: 20236–20244.

37. Fan Z, Beresford PJ, Zhang D, Lieberman J. HMG2 interacts with the nucleosome assembly protein SET and is a target of the cytotoxic T-lymphocyte protease granzyme A. *Mol Cell Biol* 2002; **22**: 2810–2820.
38. Hink-Schauer C, Estebanez-Perpina E, Wilharm E, Fuentes-Prior P, Klinkert W, Bode W *et al*. The 2.2-A crystal structure of human pro-granzyme K reveals a rigid zymogen with unusual features. *J Biol Chem* 2002; **277**: 50923–50933.
39. Simon MM, Hausmann M, Tran T, Ebnet K, Tschopp J, ThaHla R *et al*. *In vitro*- and *ex vivo*-derived cytolytic leukocytes from granzyme A × B double knockout mice are defective in granule-mediated apoptosis but not lysis of target cells. *J Exp Med* 1997; **186**: 1781–1786.
40. Voskoboinik I, Thia MC, De Bono A, Browne K, Cretney E, Jackson JT *et al*. The functional basis for hemophagocytic lymphohistiocytosis in a patient with co-inherited missense mutations in the perforin (PFN1) gene. *J Exp Med* 2004; **200**: 811–816.